Planet. Space Sci., Vol. 34, No. 10, pp. 889–901, 1986
Printed in Great Britain.

0032–0633/86 $3.00+0.00
Pergamon Journals Ltd.

STRUCTURAL AND DYNAMICAL ASPECTS OF THE DISTANT MAGNETOTAIL DETERMINED FROM ISEE-3 PLASMA MEASUREMENTS*

E. W. HONES, JR., R. D. ZWICKL, T. A. FRITZ and S. J. BAME
University of California, Los Alamos National Laboratory, Los Alamos, NM 87545, U.S.A.

(*Received* 29 *January* 1986)

Abstract—Large lateral displacements of the magnetotail at ISEE-3 orbital distances can result from the angular variations of solar wind flow that occur frequently. To determine the tail's shape and structure from the ISEE-3 measurements it is desirable to determine quantitatively the tail's displacement during such measurements. Three-dimensional solar wind measurements by IMP-8 have been used together with a new coordinate system, the Geocentric Solar Wind (GSW) system, which reflects solar wind direction changes (as well as earth dipole motion), to estimate the location of ISEE-3 within the tail cross-section. Preliminary tests suggest that at least those changes of satellite location within the tail resulting from long term (few hour) solar wind changes can be determined by the method. Energetic ion spectra, measured in plasmoids by ISEE-3 in the distant tail and by ISEE-2 at the time of the plasmoids' departure from the near tail, have the same exponential form, distinctly different from the power law form that has earlier been ascribed to plasma sheet ion spectra. The ions are trapped in the closed loops of the plasmoid and the major anisotropy that they show is due to their convective motion with the moving plasmoid, not to field-aligned streaming.

THE DISTANT MAGNETOTAIL'S RESPONSE TO CHANGES OF SOLAR WIND DIRECTION

The solar wind flows at speeds ranging from about 300 to 800 km s^{-1}; its direction frequently changes by $\pm(5\text{–}10)^\circ$ around the radial direction from the sun and changes as large as 20° sometimes occur. The magnetotail is expected to respond to changes of the solar wind flow direction, much as a windsock responds to changes of atmospheric winds, waving to and fro and suffering distortions as solar wind changes propagate along it. At distances of $\sim 220\ R_e$ where ISEE-3 spent much time observing the tail, a change of solar wind direction of 10° will deflect the tail sidewards by 35–40 R_e, more than half the tail's diameter (estimated from ISEE-3 measurements to be $\sim 60\ R_e$ at distances beyond $\sim 100\ R_e$). It is clearly important (if at all possible) to try to estimate the tail's deflection at times when ISEE-3 was making plasma, magnetic field and energetic particle measurements to develop some idea of the sizes of the different tail regions (plasma sheet, lobes, boundary regions, plasmoids etc), their spatial associations with one another and, indeed the size and shape of the tail itself.

By good fortune, three-dimensional solar wind measurements are available from the IMP-8 satellite for part of the time that ISEE-3 was exploring the magnetotail. Efforts have begun, using those data as input, to estimate the ISEE-3 location relative to the tail's axis, both in hopes of improving the understanding of the ISEE-3 tail measurements and to gain information simply on the manner in which the tail responds to solar wind changes. To conduct this effort in a meaningful way it is necessary to use a coordinate system more appropriate than the aberrated Geocentric Solar Magnetospheric (GSM) system that has commonly been used to estimate the location of ISEE-3 in the tail. The Geocentric Solar Wind (GSW) system has been developed for this purpose. Here the nature of this system and the very preliminary tests of it that have been made are reported.

THE GSW COORDINATE SYSTEM

Several different coordinate systems are used in magnetospheric studies. These coordinate systems are used to display satellite trajectories, boundary locations and vector field measurements. The system that has been most successful in ordering observational data in the outer magnetosphere, especially in the magnetotail, is the Geocentric Solar Magnetospheric (GSM) system. Its X-axis is directed from the earth toward the sun; its Z-axis is the projection of the earth's dipole axis in a plane perpendicular to the earth–sun line and the Y-axis completes the right-

---

*Invited paper presented at IAGA "Deep Tail" Symposium 1985.

handed orthogonal set. This coordinate system reflects the fact that the magnetotail is most strongly influenced by the solar wind flow (assumed radial from the sun) and by the direction of the dipole. The effects of the dipole's diurnal and annual tilt toward and away from the sun are accounted for by empirically-derived formulas (e.g. Russell and Brody, 1967) that evaluate the lifting and lowering of the neutral sheet from the GSM equational (X–Y) plane that is caused by this dipole tilt. The GSM coordinate system is depicted in Fig. 1a. The solar wind, as seen in the earth's rest frame, does not arrive radially from the sun but approaches, on the average, from $\sim$4° west of the sun because of the earth's orbital motion around the sun. To account for this "aberrated" solar wind flow, people working with ISEE-3 tail data have often simply rotated the GSM system 4° around the Z_{GSM} axis. While this represents an improvement over the GSM system itself, it is not fully correct. Instead the correct system's X-axis should be aligned anti-parallel to the aberrated solar wind flow and the dipole axis projected into a plane perpendicular to that "aberrated" X-axis; the Russell–Brody formula would then use the dipole tilt calculated in that modified system.

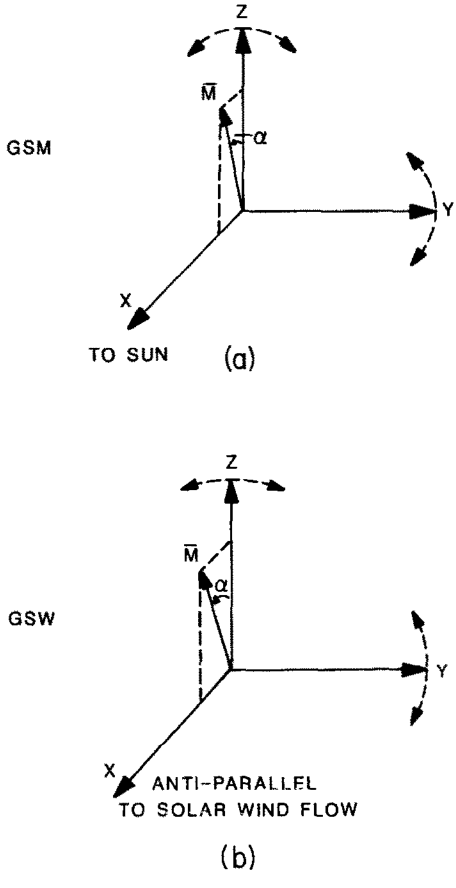

FIG. 1. THE GEOCENTRIC SOLAR MAGNETOSPHERIC (GSM) COORDINATE SYSTEM (a) AND THE GEOCENTRIC SOLAR WIND (GSW) COORDINATE SYSTEM (b). $\bar{M}$ IS THE DIRECTION OF THE EARTH'S DIPOLE AXIS WHICH LIES IN THE X–Z PLANE OF EACH COORDINATE SYSTEM, α IS THE TIME-VARYING ANGLE THAT $\bar{M}$ MAKES WITH THE Z AXIS.

If the actual direction of the solar wind flow in three dimensions is known, then a system may be used whose X-axis is aligned anti-parallel to the actual flow and whose Z-axis is the projection of the dipole axis into the plane perpendicular to X. The Russell–Brody formula would then use the dipole tilt calculated in that system. Such a system has been developed, the Geocentric Solar Wind (GSW) system, using the methods described by Russell (1971). It is depicted in Fig. 1b. The objective was to apply it to ISEE-3 distant tail measurements during the time, after mid-February 1983, when three-dimensional solar wind measurements were available from the MIT solar wind analyzer on IMP-8. Of course, in the absence of solar wind measurements, the GSW system should, at any rate, be used in place of the incorrectly modified GSM system mentioned above to correctly incorporate the assumed aberrated solar wind flow.

Even if the three-dimensional solar wind flow were measured very frequently with perfect precision, the ISEE-3 location relative to the tail axis could still be in doubt at a given instant because the nature of the tail's response to solar wind speed and direction changes is only poorly known. Figure 2 illustrates this problem. It suggests a way in which the tail's direction may evolve as the solar wind flow changes from one direction to another. The figure, furthermore, illustrates the tail response that has been assumed in the preliminary analysis of combined IMP-8/ISEE-3 data. The figure shows the section of the tail that has been engulfed by the new solar wind taking the direction of that new solar wind almost immediately, so that very soon after the front of changed solar wind flow reaches ISEE-3, the magnetotail out to the distance of ISEE-3 will be aligned with the new solar wind flow direction.

The tail response illustrated in Fig. 2 seems reasonable in the light of some studies of comet tail responses to solar wind changes. There have been two studies of such tail turning events when satellite measurements of the causative solar wind change(s) were available. The first, by Niedner *et al.* (1978), was a study of comet Kohoutek. However, most relevant to this paper was the study of comet Bradfield 1979L by Brandt *et al.* (1980) and Niedner *et al.* (1983). Figure 3 shows three pictures of that comet separated by 15.5

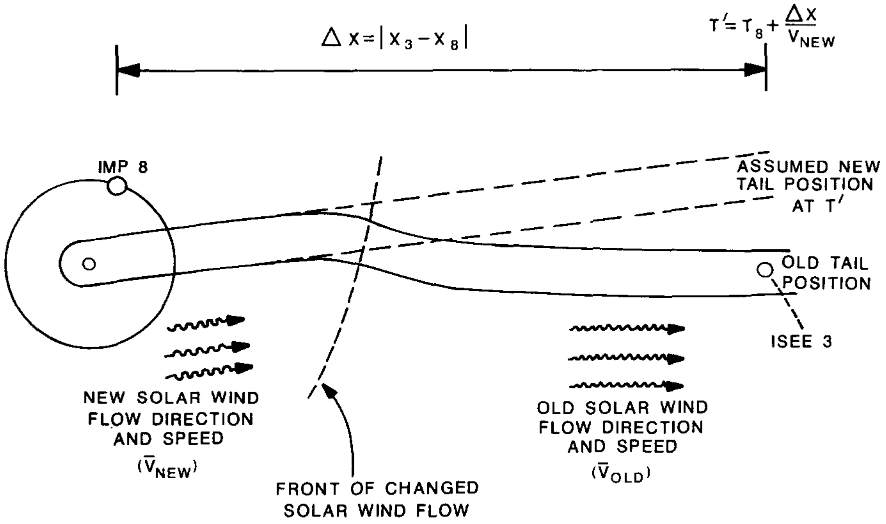

FIG. 2. ASSUMED RESPONSE OF THE MAGNETOTAIL TO A CHANGE OF SOLAR WIND DIRECTION.

and 12.0 min respectively. A distinct change of angle is seen to propagate along the tail from the comet's head. Niedner *et al.* (1983) showed that this propagating southward deflection could reasonably be ascribed to the arrival at the comet of a ~ 50 km s^{-1} southward change of the polar speed of the solar wind, which was observed about 12 h earlier by Helios 2, 0.15 AU directly upstream of the comet. It is interesting to note the 10^6 km scale in the pictures in Fig. 3 and to recall that the ISEE-3 apogee was 1.5×10^6 km down-tail from the earth.

Niedner *et al.* (1983) remarked that their study of comet Bradfield clearly underscored the sensitivity of comet plasma tails to sudden large-scale changes in the bulk flow of the solar wind. The fact that the earth's magnetotail probably is similarly sensitive indicates the need, in analyzing the ISEE-3 distant tail data, to try to determine the satellite's location in a coordinate system that correctly reflects solar wind changes. Figure 4 shows the results of the authors' preliminary testing of the GSW system. Choosing a 4-day interval in July 1983 when ISEE-3 was 235 R_e down-tail and quite near the nominal center of the tail in both the Y and Z directions, 10-min averages of the solar wind flow magnitude and its ecliptic latitude and longitude were made, which were obtained from the IMP-8 satellite. Using the solar wind speed and the IMP-8/ISEE-3 separation in the GSE X direction the approximate arrival time at ISEE-3 of each 10-min sample of solar wind was determined (see Fig. 2). It was assumed, then, that the tail axis all the way from the earth to ISEE-3 had the direction of each solar wind sample as it arrived at ISEE-3 and the ISEE-3 location was calculated in the GSW coordinate system. This assumption is an obvious over simplification if the solar wind direction varies on a time scale shorter than the IMP-8/ISEE-3 travel time. For longer times the comet behavior in Fig. 3 suggests that the assumption might be reasonable.

The Y_{GSW} and Z_{GSW} positions of ISEE-3 are plotted in Fig. 4 for the 4 days. (The Russell–Brody correction for dipole tilt toward the sun was not used in these calculations because its applicability at such large distances has not been tested.) The dashed lines in the Y_{GSW} and Z_{GSW} panels are the coordinates of ISEE-3 in the GSW system but calculated with simply a constant solar wind aberration angle of 4°. Hereafter the locations shown by these lines will be referred to as Y'_{GSW} and Z'_{GSW}. In the bottom panels the "region identifier" for ISEE-3 derived from ISEE-3 plasma and magnetic field data is shown (Zwickl *et al.*, 1984). This parameter tells whether the satellite is thought to be in the plasma sheet (PS), north lobe or south lobe (NL, SL) or in the magnetosheath (MS) outside the north lobe (top) or outside the south lobe (bottom). The object of Fig. 4 is to determine how well the region identifier agrees with the environment expected from the satellite's calculated GSW coordinates. The most meaningful comparison that can be made is between the north–south variations of the region identifier and the calculated Z_{GSW} (or Z'_{GSW}) position.

First note that the Y'_{GSW} and Z'_{GSW} positions of ISEE-3 change hardly at all during the 4-day interval, yet the region identifier indicates that the satellite environment ranged from the south magnetosheath through the north lobe. Clearly Z'_{GSW} has little relevance to the satellite's location relative to actual tail boundaries. Z_{GSW}, however, does seem to display correlations with region changes on a few-hour time scale. Notice that throughout 10 July ISEE-3 was mostly in the south magnetosheath or south lobe. During that time Z_{GSW} was quite strongly negative. In the first half of 11 July and the last 3 h of that day, ISEE-3 was often in the plasma sheet and even in the north lobe. Z_{GSW} ranged around zero and even became strongly positive sometimes. After 1400 UT on 12 July, ISEE-3 was mostly in the south magnetosheath and during most of that time Z_{GSW} was strongly negative. There are a few indications that correlation on a shorter time scale may occur. For example, dips of Z_{GSM} to very large negative values on 10 July at ~0530 UT, ~0800 UT and ~1100 UT coincide with excursions of ISEE-3 into the south magnetosheath.

These results demonstrate an up-and-down waving motion of the magnetotail occurring in response to north–south variations of the solar wind direction and show that the two phenomena can be related in at least a semi-quantitative fashion by using 3-dimensional solar wind measurements in conjunction with the appropriate (GSW) coordinate system. Much more work needs to be done, comparing ISEE-3 environment and changes of environment with the measured solar wind, if the magnetotail's response to solar wind changes is to be clearly perceived. Unfortunately there are only about 6 months of concurrent data and many gaps appear in both data sets.

This first study of the magnetotail's motion in response to the actual 3-dimensional flow of the solar wind demonstrates that such motion does occur in roughly the expected fashion and can be noted from within the tail itself. Furthermore, it demonstrates the need for accurate, continual 3-dimensional solar wind measurements to be made in support of future satellite observations in the distant magnetotail, e.g. those planned as part of the International Solar Terrestrial Physics (ISTP) program. (It may be necessary that the solar wind measurements be made far upstream of the magnetosphere to avoid the effects of the foreshock.) Without such supporting measurements it will be impossible to reliably determine the structure and dimensions of the distant tail.

ENERGETIC IONS IN THE PLASMA SHEET

Energetic ions and electrons populate the plasma sheet and are found in varying intensities, being most intense during geomagnetically active times. Measurements in the near-earth (~30–40R_e) region of the plasma sheet have been reported that showed the energetic ions to constitute a high energy (> 50 keV) tail with differential energy spectral form, $CE^{-\gamma}$, that joins smoothly onto a Maxwellian spectrum that prevails at lower energies (Sarris *et al.*, 1981). Williams (1981), using particle data measured with ISEE-1 near times of crossing of the plasma sheet–lobe boundary, noted that the ion angular distribution was beam-like, directed along the magnetic field, or at other angles to the field. He concurred in the general spectral form found by Sarris *et al.* (1981) and proposed that the beam-like aspects of the distributions could all be explained in terms of single-particle motion of the ions.

Much farther down-tail the ISEE-3 encounters with the plasma sheet often were the result of the passage of plasmoids, the disconnected plasma sheet segments that are created at substorm onset and that leave the magnetotail at high speed (Hones, 1979; Hones *et al.*, 1984a, b; Scholer *et al.*, 1984). Gloeckler *et al.* (1984a, b) measured velocity distributions of ions in the rest frame of the moving plasmoids and found them to be different than those mentioned above. Hones *et al.* (1986) found a similar ion velocity distribution in a plasmoid as it was leaving the near-earth tail. Here these energetic ion measurements in the distant and near magnetotail and some implications regarding their source are discussed.

ISEE-3 MEASUREMENTS OF ION SPECTRA IN PLASMOIDS

At the onset of a substorm's expansive phase, a longitudinal sector of the plasma sheet, comprising perhaps a third to a half of the plasma sheet's cross-tail width, is severed from earth by magnetic reconnection, forming a plasmoid, i.e. a structure of closed magnetic loops, which then retreats down-tail at speeds of 500–1000 km s^{-1}. Also, beginning at expansive phase onset, energetic electrons and ions seem somehow to be generated and to populate the plasma sheet as well as the inner regions of the magnetosphere. Possibly these are also a consequence of the magnetic reconnection process. Some of the energetic particles are trapped in the plasmoid and are carried down-tail within it. Others continue to be accelerated after the plasmoid has departed. These populate the open field lines of the separatrix layer (Hones, 1984a) and the post-plasmoid plasma sheet that envelops the plasmoid as it leaves.

The energetic particles within the plasmoids and in the regions surrounding them have played a very important role, first in the initial identification of plasmoids near earth (Hones, 1979; Bieber *et al.*, 1982)

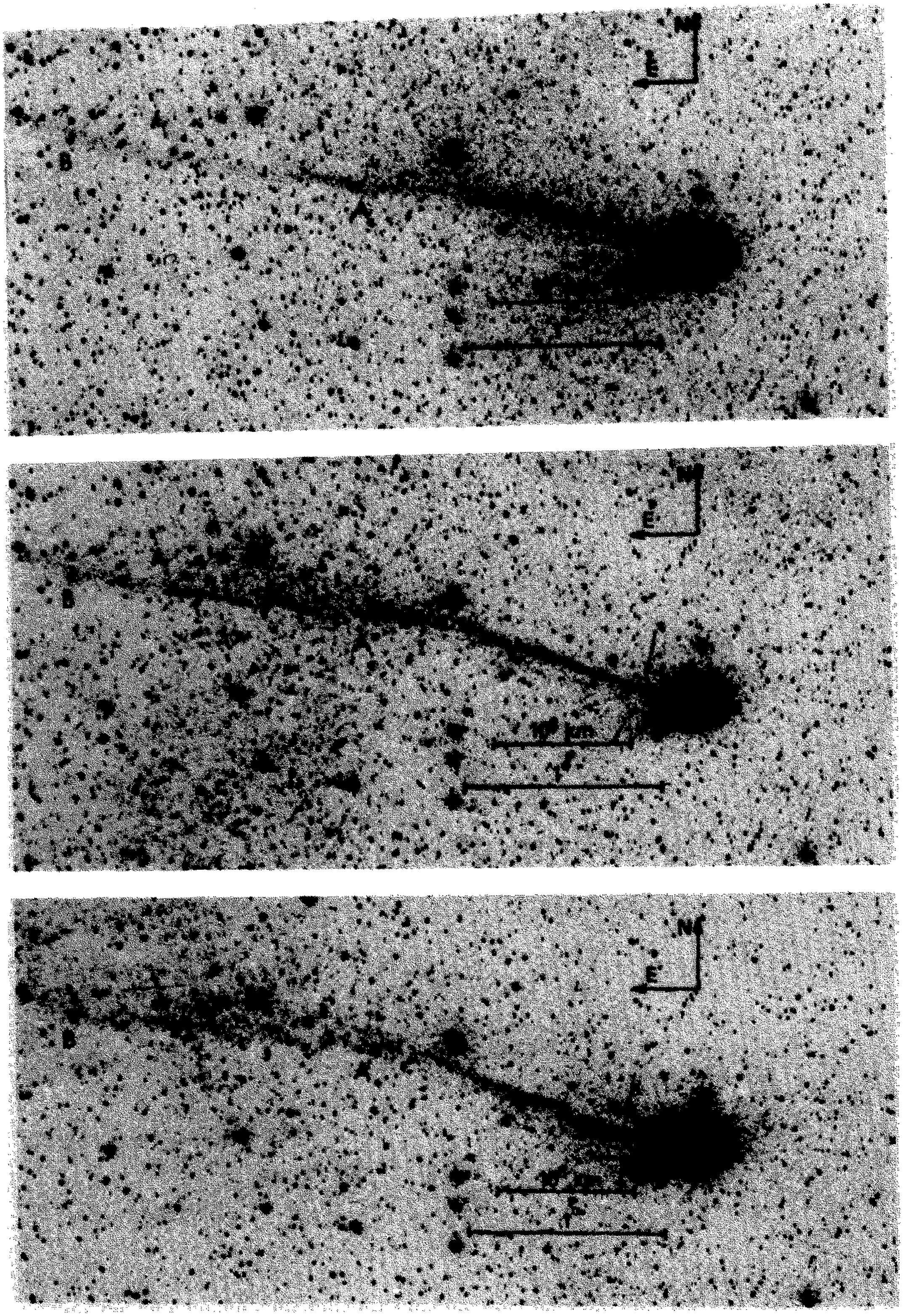

Fig. 3. Photographs of comet Bradfield 1979L showing the effect of a direction change of the solar wind. The pictures were taken on 6 February 1980 at 02:32:30 UT, 02:48:00 UT and 03:00:00 UT. Arrows indicate the bend of the tail caused by the solar wind change. (From Brandt *et al.*, 1980.)

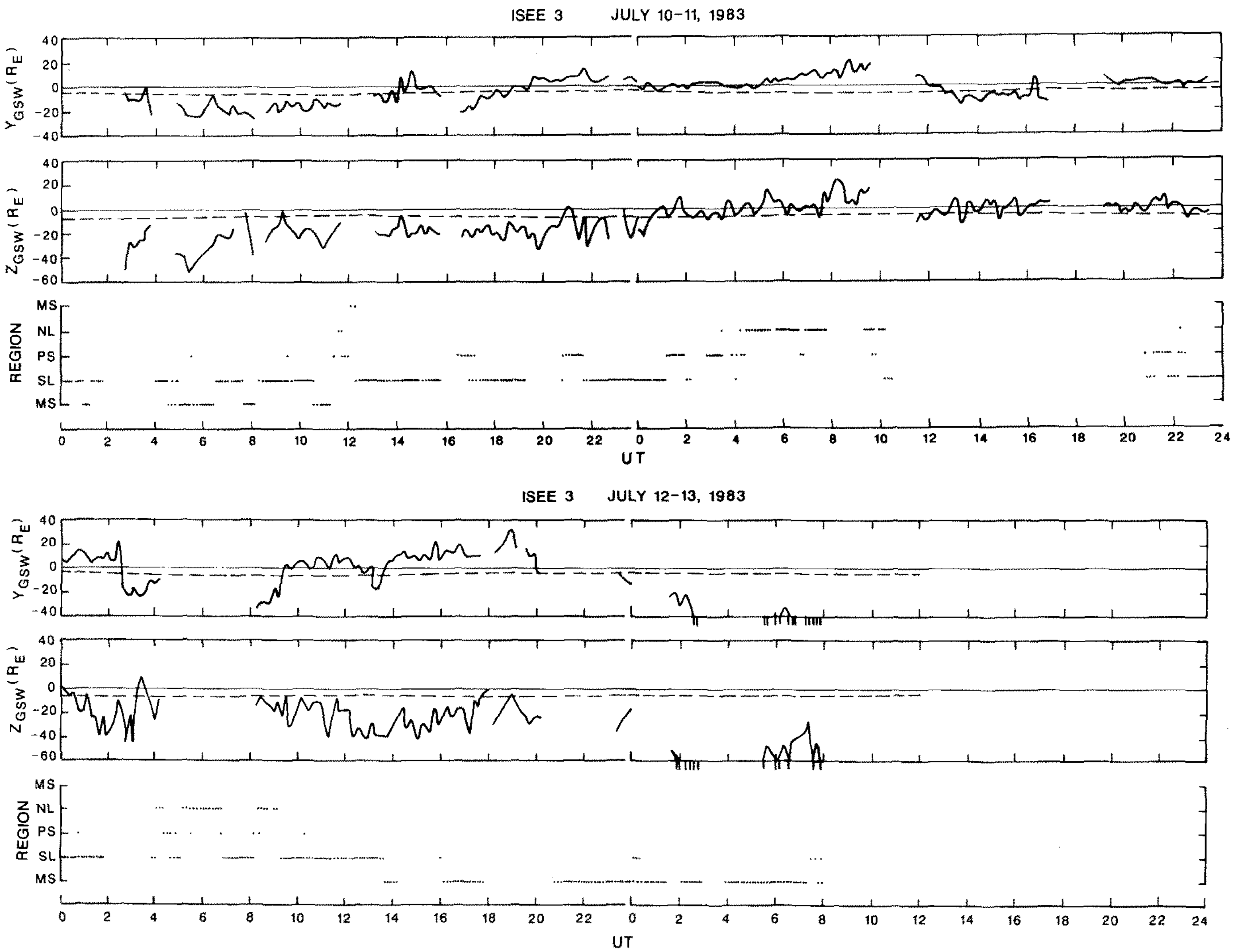

FIG. 4. Y_{GSW} AND Z_{GSW} COORDINATES OF ISEE-3, 10–13 JULY 1983. X_{GSW} WAS ~ −235 R_e. THE SOLID LINES IN THE Y_{GSW} AND Z_{GSW} PANELS WERE DERIVED USING THE MEASURED 3-D SOLAR WIND FLOW AS DESCRIBED IN THE TEXT. THE DASHED LINES WERE DERIVED ASSUMING A CONSTANT 4° ABERRATION ANGLE. THE BOTTOM PANEL SHOWS THE REGION IDENTIFIER DEDUCED FROM ISEE-3 PLASMA AND FIELD MEASUREMENTS.

and later in the recognition of them passing ISEE-3 in the distant tail (Hones *et al.*, 1984a; Scholer *et al.*, 1984).

Gloeckler *et al.* (1984a) reported an interesting observation of energetic ions in a plasmoid that passed ISEE-3 216 R_e down-tail on 16 February 1983. (Other aspects of that same plasmoid were reported by Hones *et al.* (1984b).) They used measurements of energy per unit charge (E/q) of protons and alpha particles at three energies (~30, ~60 and ~120 keV/e) and at eight azimuthal angles. They used an iterative process to transform the measured ion distribution function from the satellite rest frame to the plasmoid rest frame. For this they assumed that (a) protons and alpha particles are carried along by the plasmoid at a common flow velocity and (b) the velocity distribution function, $f(v)$, for each species is isotropic in the plasmoid rest frame. By using different assumed flow vel-

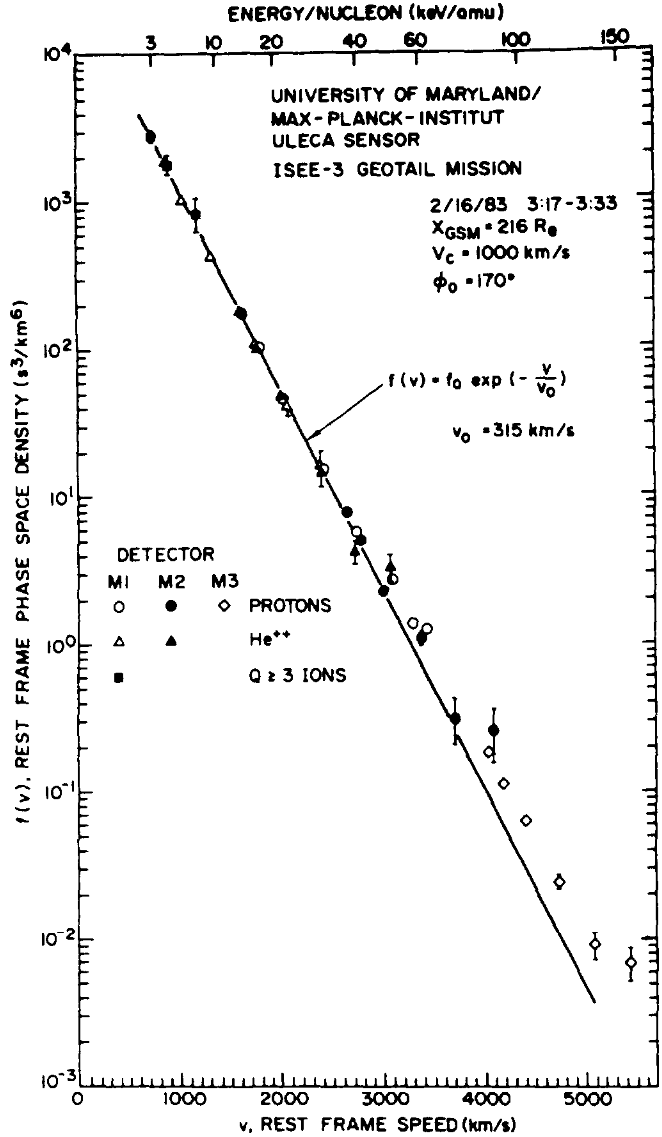

FIG. 5. REST FRAME DISTRIBUTION FUNCTIONS, $f(v)$, FOR SUPRATHERMAL H^+, He^{2+} AND ($Q \geqslant 3$) HEAVY IONS VS v, THE ION SPEED. f_{He} AND $f_{(Q \geqslant 3)}$ HAVE BEEN MULTIPLIED BY 30 AND 530, RESPECTIVELY. (FROM GLOECKLER *et al.*, 1984a.)

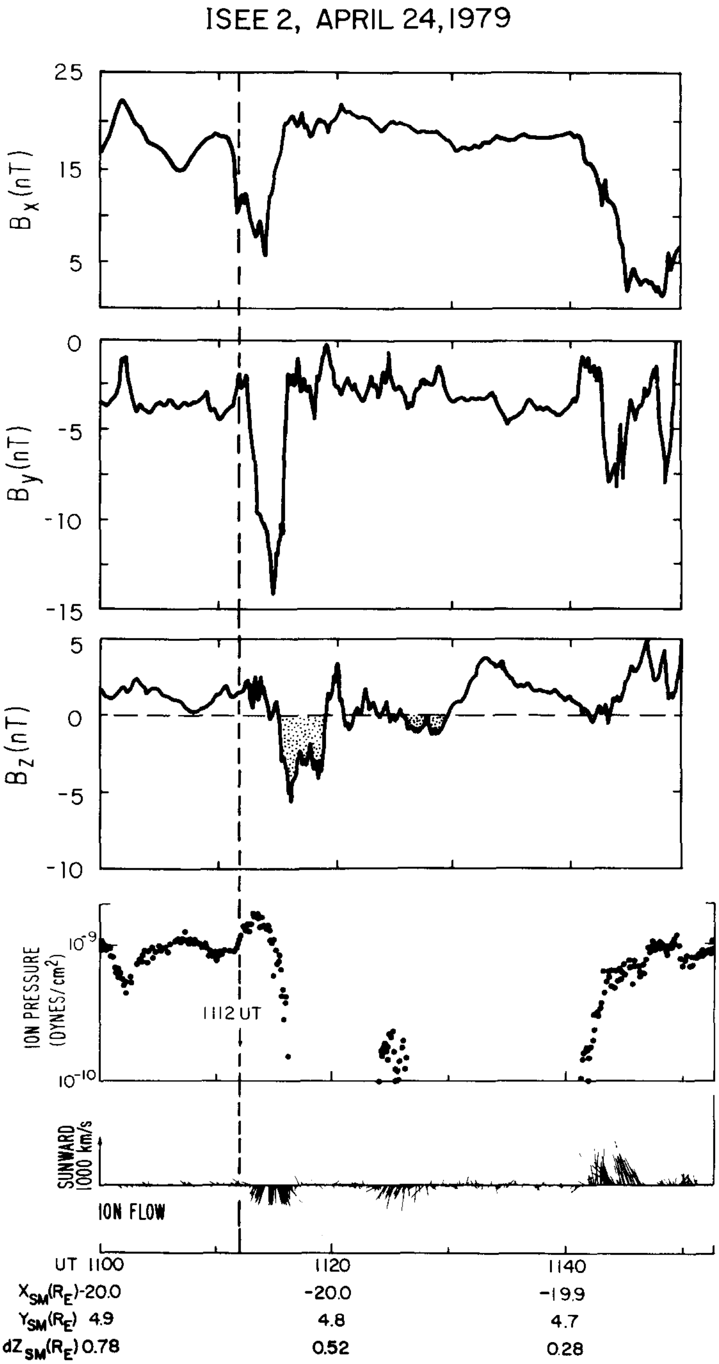

FIG. 6. MAGNETIC FIELD AND PLASMA PARAMETERS MEASURED BY ISEE-2 DURING THE 24 APRIL 1979 SUBSTORM. THE BOTTOM PANEL PRESENTS VECTORS SHOWING THE MAGNITUDE AND DIRECTION OF PLASMA ION BULK FLOW. THE ARROW AT THE LEFT INDICATES A BULK FLOW OF 1000 km s^{-1} DIRECTED SUNWARD. DUSKWARD FLOW IS TOWARD THE LEFT AND DAWNWARD IS TOWARD THE RIGHT. SUBSTORM ONSET AT 1112 UT IS INDICATED. THE SATELLITE LOCATION IS SHOWN AT THE BOTTOM. (FROM HONES *et al.*, 1986.)

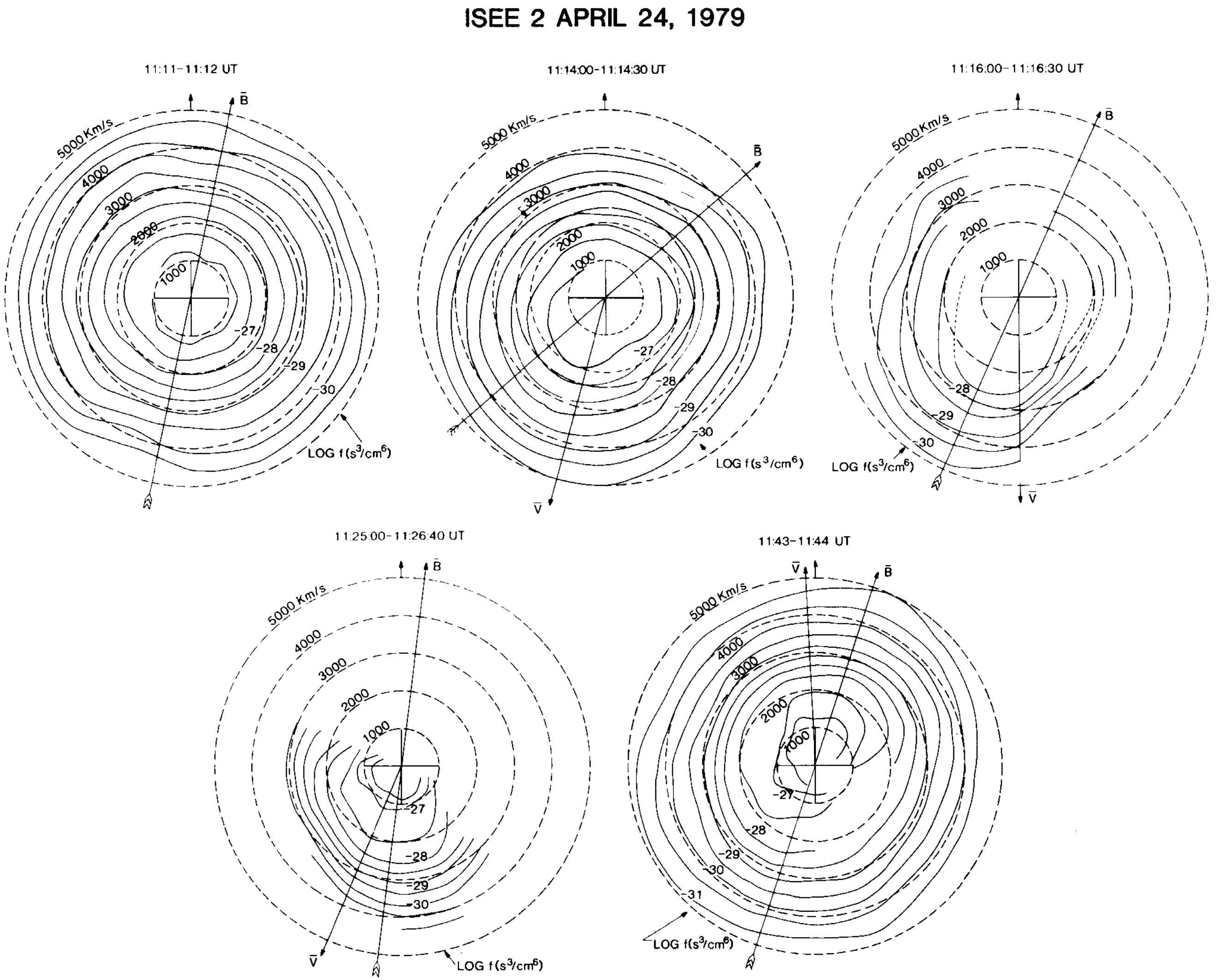

FIG. 7. TWO DIMENSIONAL VELOCITY DISTRIBUTION FUNCTIONS OF IONS MEASURED WITH A PLASMA ANALYZER AND WITH A MEDIUM ENERGY PARTICLE DETECTOR ON ISEE-2. CONTOURS ARE DRAWN AT INTERVALS OF $\sqrt{10}$ IN PHASE SPACE DENSITY, f. DATA FROM THE PLASMA ANALYZER COVER THE VELOCITY RANGE UP TO 2400 km s^{-1}. THE AVERAGE DIRECTION OF THE MAGNETIC FIELD, $\bar{B}$, IS SHOWN AS IS THE DIRECTION OF THE VELOCITY, $\bar{v}$, DERIVED FROM THE FIRST MOMENT OF THE DISTRIBUTION FUNCTION MEASURED BY THE PLASMA ANALYZER. (FROM HONES *et al.*, 1986.)

ocities in the transformation they found a magnitude and direction of flow that caused all the measured intensities to line up on a common curve of log $f(v)$ vs v. That curve (see Fig. 5) turned out to be a straight line, implying an exponential velocity distribution $f(v) = f_0 e^{-v/v_0}$, with $v_0 = 315$ km s^{-1}. The plasmoid velocity, v_c, that provided this best fit was 1000 km s^{-1} toward solar ecliptic azimuth, $\phi_0 = 170°$, in good agreement with the plasma bulk flow velocity measured at the same time with the Los Alamos plasma electron instrument on ISEE-3 (Hones *et al.*, 1984b).

Later, repeating this analysis for 20 previously identified plasmoids, Gloeckler *et al.* (1984b) found, in each case, an exponential velocity distribution. From case to case, v_0 varied but averaged 380 km s^{-1} for protons and 340 km s^{-1} for alpha particles.

ISEE-2 MEASUREMENTS OF ION SPECTRA IN A FORMING PLASMOID

Hones *et al.* (1986) conducted a study of the plasma sheet at $r \approx 20$ R$_e$ during a substorm that included detailed analyses of ions at seven energies from ~25 to 125 keV. The response of the plasma sheet to this substorm, whose expansive phase began at 1112 UT on 24 April 1979, is shown in Fig. 6. A drop out of the plasma sheet ion flux occurred within about 4 min after substorm onset, accompanied by southward-turning B_z and fast tailward flow of plasma. Figure 7 shows 2-dimensional distribution functions of ions over the velocity range ~1000–5000 km s^{-1} constructed for several intervals during the substorm. The distribution function for 11 : 14 : 00–11 : 14 : 30 UT,

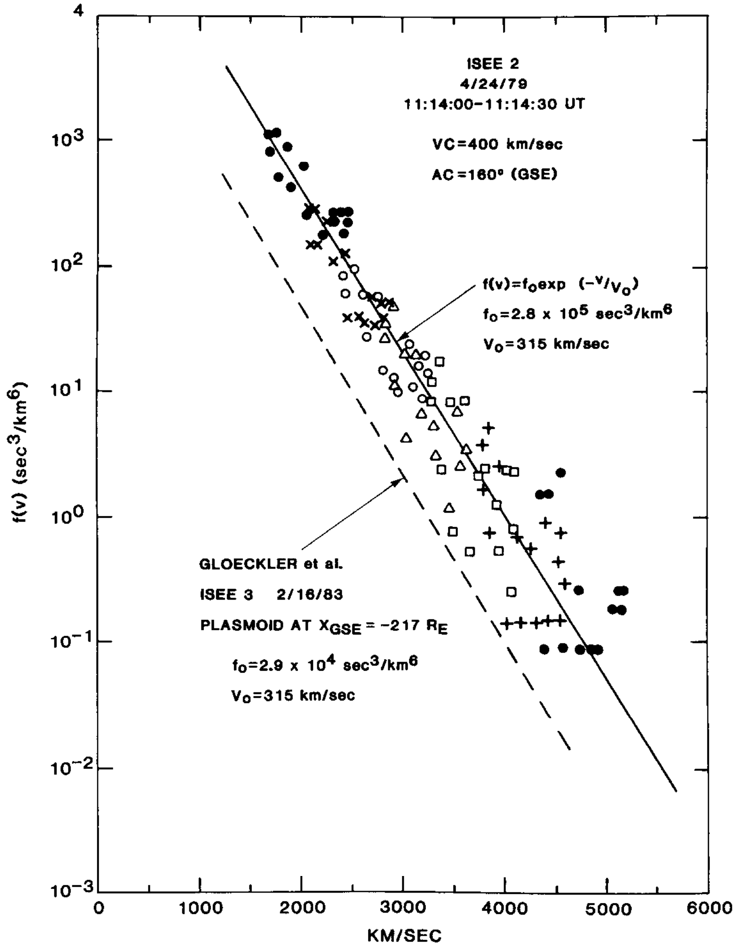

FIG. 8. REST FRAME DISTRIBUTION FUNCTION, $f(v)$, FOR IONS VS v, THE ION SPEED, FOR THE 11 : 14 : 00–1 : 14 : 30 UT DATA SHOWN IN FIG. 7. THE DIFFERENT SYMBOLS REPRESENT THE SEVEN DIFFERENTIAL ENERGY RANGES OF THE DETECTOR ; MEASUREMENTS AT 16 AZIMUTHAL ANGLES WERE MADE AT EACH ENERGY.

UT, measured as the plasma intensity was decreasing and about a minute before B_z turned southward, is assumed to have been measured in the plasmoid as it was being formed and starting its journey down-tail. Note that two types of anisotropy appear in this distribution: (a) an elongation along B with a net displacement of contours in the tailward sense along B; and (b) a displacement of all contours nearly in the anti-sunward direction, along the velocity vector, V, derived from the plasma ion (E_i = 100–30,000 eV) measurements. The anisotropy (a) can be thought to be due to ion motion back and forth along the magnetic field (i.e. the single-particle interpretation of Williams), but the anisotropy (b) is due to the convective motion of the ions with the plasma in the tailward-departing plasmoid within which they are trapped. This very substantial component is not amenable to a single-particle interpretation but is due to the collective motion of the ions with the plasma.

The energetic (25–125 keV) ions in the 11:14:00–11:14:30 distribution were transformed to the plasmoid rest frame using the measured flow velocity (400 km s^{-1} at $\phi_{GSE} = 160°$) of the plasma ions and assuming their distribution in the plasmoid frame was isotropic. (A slightly elliptical distribution, suggested by Fig. 7, should perhaps have been assumed for this transformation.) The velocity spectrum in the plasmoid frame is shown in Fig. 8. It is seen to be quite well fit by a straight line, which implies an exponential dependence of $f(v)$ on v, with v_0 = 315 km s^{-1}. The data are not well fit by the $E^{-\gamma}$ curves shown, for example in Fig. 7 of Williams (1981). On the other hand, they differ from the results of Gloeckler *et al.* (1984a) only in their absolute magnitude, the ISEE-2 data implying about 10 times greater intensity at all velocities.

These energetic ion results, both from ISEE-2 and from ISEE-3, show that a major anisotropy of the flux is due to bulk motion of the ions with the moving plasma of the plasmoid. Furthermore the ion spectrum is very closely an exponential variation of $f(v)$ with v and is not well fit by a power law in energy. These results clearly contrast with those of Williams (1981), but Williams' results came from one set of observations and seem to apply specifically to the lobe–plasma sheet interface region. Possibly conditions of the ions within plasmoids are systematically different from those elsewhere. On the other hand, it would seem that the spectrum of ions trapped within plasmoids might be quite similar to the primary source spectrum if, as seems possible, the ions are both energized and trapped in the plasmoid by the act of magnetic reconnection that forms the plasmoid.

It is interesting to note that computer simulations have shown that test particles accelerated by turbulent magnetohydrodynamic reconnection (Matthaeus *et al.*, 1984) have been found to show an exponential variation of $f(v)$ with v. Furthermore, values of v_0 found in those computer simulations are not inconsistent with the values ($\sim$300–400 km s^{-1}) actually observed in the magnetotail (W. H. Matthaeus, private communication, 1985).

Acknowledgments—The authors are grateful to A. J. Lazarus for providing solar wind data from the MIT solar wind instrument on IMP-8. This work was done under the auspices of the U.S. Department of Energy.

REFERENCES

Bieber, J. W., Stone, E. C., Hones, E. W., Jr., Baker, D. N. and Bame, S. J. (1982) Plasma behavior during energetic electron streaming events: further evidence for substorm-associated magnetic reconnection. *Geophys. Res. Lett.* **9**, 664.

Brandt, J. C., Hawley, J. D. and Niedner, M. B., Jr. (1980) A very rapid turning of the plasma-tail axis of comet Bradfield 1979L on 1980 February 6. *Ap. J.* **241**, L51–L54.

Gloeckler, G., Scholer, M., Ipavich, F. M., Hovestadt, D., Klecker, B. and Galvin, A. B. (1984a) Abundances and spectra of suprathermal H^+, He^{++} and heavy ions in a fast moving plasma structure (plasmoid) in the distant geotail. *Geophys. Res. Lett.* **11**, 603.

Gloeckler, G., Ipavich, F. M., Hovestadt, D., Scholer, M., Galvin, A. B. and Klecker, B. (1984b) Characteristics of suprathermal H^+ and He^{++} in plasmoids in the distant magnetotail. *Geophys. Res. Lett.* **11**, 1030.

Hones, E. W., Jr. (1979) Transient phenomena in the magnetotail and their relation to substorms. *Space Sci. Rev.* **23**, 393.

Hones, E. W., Jr., Baker, D. N., Bame, S. J., Feldman, W. C., Gosling, J. T., McComas, D. J., Zwickl, R. D., Slavin, J., Smith, E. J. and Tsurutani, B. T. (1984a) Structure of the magnetotail at 220 R_e and its response to geomagnetic activity. *Geophys. Res. Lett.* **11**, 5.

Hones, E. W., Jr., Birn, J., Baker, D. N., Bame, S. J., Feldman, W. C., McComas, D. J., Zwickl, R. D., Slavin, J. A., Smith, E. J. and Tsurutani, B. T. (1984b) Detailed examination of a plasmoid in the distant magnetotail with ISEE-3. *Geophys. Res. Lett.* **11**, 1046.

Hones, E. W., Jr., Fritz, T. A., Birn, J., Cooney, J. and Bame, S. J. (1986) Detailed observations of the plasma sheet during a substorm on April 24, 1979. *J. geophys. Res.* **91**, 6845.

Matthaeus, W. H., Ambrosiano, J. J. and Goldstein, M. L. (1984) Particle acceleration by turbulent magnetohydrodynamic reconnection. *Phys. Rev. Lett.* **53**, 1449.

Niedner, M. B., Jr., Brandt, J. C., Zwickl, R. D. and Bame, S. J. (1983) Interaction of the plasma tail of comet Bradfield 1979L on 1980 February 6 with a possibly flare-generated solar-wind disturbance, in *Solar Wind Five*, NASA Conference Publication 2280 (Edited by Neugebauer, M.), p. 737. NASA Scientific and Technical Information Branch, Washington, D.C.

Russell, C. T. (1971) Geophysical coordinate transformations. *Cosmic Electrodynam.* **2**, 184.

Russell, C. T. and Brody, K. I. (1967) Some remarks on the position and shape of the neutral sheet. *J. geophys. Res.* **72**, 6104.

Sarris, E. T., Krimigis, S. M., Lui, A. T. Y., Ackerson, K. L., Frank, L. A. and Williams, D. J. (1981) Relationship between energetic particles and plasmas in the distant plasma sheet. *Geophys. Res. Lett.* **8**, 349.

Scholer, M., Gloeckler, G., Klecker, B., Ipavich, F. M., Hovestadt, D. and Smith, E. J. (1984) Fast moving plasma structures in the distant magnetotail. *J. geophys. Res.* **89**, 6717.

Williams, D. J. (1981) Energetic ion beams at the edge of the plasma sheet: ISEE-1 observations plus a simple explanatory model. *J. geophys. Res.* **86**, 5507.

Zwickl, R. D., Baker, D. N., Bame, S. J., Feldman, W. C., Gosling, J. T., Hones, E. W., Jr. and McComas, D. J. (1984) Evolution of the earth's distant magnetotail: ISEE-3 electron plasma results. *J. geophys. Res.* **89**, 11007.